# ARTICLE

# Catalyst-TiO(OH)$_2$ could drastically reduce the energy consumption of CO$_2$ capture

Qinghua Lai [1], Sam Toan[1], Mohammed A. Assiri[2], Huaigang Cheng[1], Armistead G. Russell[3], Hertanto Adidharma[1], Maciej Radosz[1] & Maohong Fan[1,3,4]

Implementing Paris Climate Accord is inhibited by the high energy consumption of the state-of-the-art CO$_2$ capture technologies due to the notoriously slow kinetics in CO$_2$ desorption step of CO$_2$ capture. To address the challenge, here we report that nanostructured TiO(OH)$_2$ as a catalyst is capable of drastically increasing the rates of CO$_2$ desorption from spent monoethanolamine (MEA) by over 4500%. This discovery makes CO$_2$ capture successful at much lower temperatures, which not only dramatically reduces energy consumption but also amine losses and prevents emission of carcinogenic amine-decomposition byproducts. The catalytic effect of TiO(OH)$_2$ is observed with Raman characterization. The stabilities of the catalyst and MEA are confirmed with 50 cyclic CO$_2$ sorption and sorption. A possible mechanism is proposed for the TiO(OH)$_2$-catalyzed CO$_2$ capture. TiO(OH)$_2$ could be a key to the future success of Paris Climat e Accord.

[1] College of Engineering and Applied Sciences, University of Wyoming, Laramie, WY 82071, USA. [2] College of Arts and Sciences, University of Wyoming, Laramie, WY 82071, USA. [3] School of Civil and Environmental Engineering, Georgia Institute of Technology, Atlanta, GA 30332, USA. [4] School of Energy Resources, University of Wyoming, Laramie, WY 82071, USA. These authors contributed equally: Qinghua Lai, Sam Toan. Correspondence and requests for materials should be addressed to M.F. (email: mfan@uwyo.edu)

Carbon-based fuels have sustained the world for many centuries. However, their uses have resulted in large amounts of $CO_2$ emission, a likely cause of the increasingly noticeable climate changes[1–4]. Thus, $CO_2$ emission control is imperative by the Paris Climate Accord[5,6]. Chemisorption is the most selective and thus promising technology for capturing $CO_2$ emitted from fossil flue gas due to its simplicity and unique flexibility in dealing with wide concentrations and volumes of $CO_2$-containing gases[7–9]. However, its shortcomings are also obvious, including slow sorption and desorption rates. The desorption kinetics is much more important because the $CO_2$ desorption step typically is much slower and more energy-intensive than the sorption step in the overall $CO_2$ capture processes. The $CO_2$ desorption step in conventional $CO_2$ capture technologies has to be operated at higher temperatures for achieving higher reaction kinetics, typically above 100 °C, which makes this step very expensive, primarily due to the high specific and latent heat capacities of water[10].

How can the absorbed $CO_2$ be desorbed quickly at temperatures lower than 100 °C—the critical temperature for lowering energy consumption? If the use of catalyst can drastically enhance desorption rates, and thus allow for reducing the $CO_2$ desorption temperatures, such low desorption temperatures would allow not only for reducing the energy consumption but also utilizing the existing flue-gas waste heat or solar-heated-water, which could completely eliminate the extra energy sources otherwise needed for conventional above 100 °C-desorption based $CO_2$ capture technologies.

A few studies have shown that inorganic materials could be used as catalysts for $CO_2$ capture. Our group have showed that FeOOH and $TiO(OH)_2$ could be used as catalytic supports to reduce the activation energy of the $NaHCO_3$ decomposition reaction and then enhance the decomposition rate[11,12]. Idem et al. reported that H-ZSM and $\gamma$-$Al_2O_3$ could be used to accelerate the amine based solvent regeneration and thus reducing the heat duty for amine regeneration[13,14]. Bhatti et al.[15] recently reported an inspiring finding that transition metal oxides could affect spent monoethanolamine (MEA) regeneration. Two of those materials, $MoO_3$ and $V_2O_5$, were found to improve desorption rates substantially because, in fact, they react and dissolve in the $CO_2$-rich MEA solvent. For this reason, they cannot act as a classic, reusable catalyst. The other oxides investigated in that work, including $TiO_2$, had only marginal effects.

In this work, we find a fundamentally different catalyst in structure—$TiO(OH)_2$ that can radically change the pathway and thus lower the energy of $CO_2$ capture. $TiO(OH)_2$ turns out to be not only very effective in accelerating $CO_2$ desorption—the key step in $CO_2$ capture, but also quite stable, and thus a cost-effective $CO_2$ capture catalyst. A proton transfer based catalytic $CO_2$ capture mechanism is proposed. Also, the catalysis function of $TiO(OH)_2$ is supported with both $CO_2$ desorption experiments and characterization results.

## Results

**Catalytic effect of $TiO(OH)_2$ on $CO_2$ absorption and desorption.** The catalytic effect of $TiO(OH)_2$ on $CO_2$ absorption, sorption for short, and desorption using MEA solution as an example is examined in this work with a setup shown in
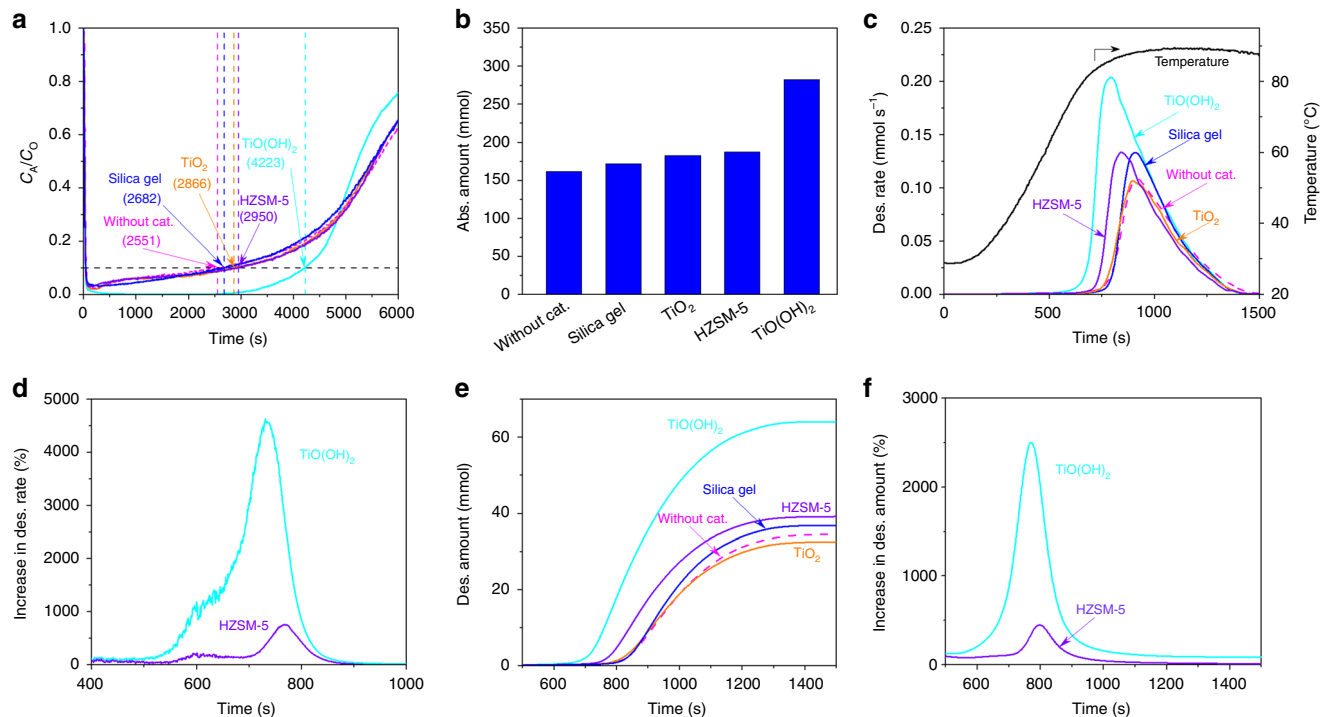


**Fig. 1** Effect of $TiO(OH)_2$ catalyst on $CO_2$ absorption (abs.) and desorption (des.). **a** Uncatalyzed and catalyzed $CO_2$ absorption profiles of 20 wt% MEA solution. **b** The quantities of the $CO_2$ sorbed within the effective absorption time (>90% $CO_2$ capture). **c** The rates of $CO_2$ desorption from spent 20 wt% MEA sorbent without and with uses of catalyst (cat.). **d** The percentage increases in $CO_2$ desorption rate due to the use of $TiO(OH)_2$. **e** Effects of $TiO(OH)_2$ on the quantities of desorbed $CO_2$. **f** The percentage increases in $CO_2$ desorption amount due to the use of $TiO(OH)_2$. Absorption conditions—total mass of solution: 200 g; MEA concentration in the solution: 20 wt%; total flow rate of gas: 1000 mL/min; composition of gas: 10 vol% $CO_2$, 10 vol% $O_2$, and 80 vol% $N_2$; temperature: 25 °C; absorption time: 6000 s. Desorption conditions—Total mass of solution: 200 g; MEA concentration in the solution: 20 wt%; temperature: 88 °C; time: 2400 s

Supplementary Fig. 1 using synthetic flue gas mixture with 10 vol % $CO_2$, 10 vol% $O_2$, and 80 vol% $N_2$. An optimal dosage (Supplementary Fig. 2) of 2 wt% $TiO(OH)_2$ is used for all the tests. Figure 1a presents $CO_2$ breakthrough curves for a 20 wt% MEA with and without $TiO(OH)_2$, HZSM-5, silica gel, and $TiO_2$, all at 2 wt%. Silica gel with similar particle size and porosity to $TiO(OH)_2$ barely changes the $CO_2$ sorption breakthrough profile. Qualitatively consistent with the Bhatti et al. work[15], $TiO_2$ also barely changes the $CO_2$ sorption breakthrough curve. Also, recently reported H-ZSM5[13,14] does not change $CO_2$ breakthrough curve much. However, $TiO(OH)_2$ significantly increases the effective sorption period in which capturing 90% $CO_2$ in flue gas is realized as targeted by U.S. Department of Energy (DOE)[16]. The sorbent with longer effective period means that it has higher sorption efficiency and faster $CO_2$ sorption. The effective sorption time without use of any catalyst and with the use of silica gel, $TiO_2$, and HZSM-5 are only 2551, 2682, 2866, and 2950 s, respectively, ~12–16 % increase. While, the period due to use of $TiO(OH)_2$ jumps to 4223 s, an increase by ~66% in comparison with that without catalyst. Accordingly, the quantities of the $CO_2$ absorbed without and with uses of $TiO(OH)_2$ within the corresponding effective sorption times are 162 and 283 mmol, respectively, as presented in Fig. 1b. This represents a 75% improvement.

The catalyst effect of $TiO(OH)_2$ on $CO_2$ desorption is evaluated with the spent MEA sorbent resulting from 6000 s of $CO_2$ sorption (Fig. 1a). The $CO_2$ desorption study is conducted by heating the $CO_2$ spent MEA sorbent to a desired desorption temperature under the given heating profile shown in the right y-axis of Fig. 1c. The left y-axis of Fig. 1c shows the changes of the rates of $CO_2$ desorption from spent 20 wt% MEA sorbent without and with uses of catalysts with time under the same temperatures. As shown in Fig. 1c, $TiO_2$ barley changes $CO_2$ desorption from the spent MEA sorbent. Unlike $TiO_2$, the HZSM-5 can slightly improve $CO_2$ desorption as reported by Idem et al.[13]. Silica gel also can slightly improve $CO_2$ desorption, however it cannot lower the temperature for maximum $CO_2$ desorption rate (Supplementary Table 1). Compared to the spent MEA without addition of the catalyst, the spent MEA with addition of $TiO(OH)_2$ could desorb much more $CO_2$ at the same low temperature range, and have a higher desorption rate at low temperatures. The highest desorption rate of spent MEA with the presence of $TiO(OH)_2$ reaches 0.204 mmol s$^{-1}$ at as early as 792 s (Supplementary Table 1), while the desorption rates of spent MEAs without the use of $TiO(OH)_2$ and with the use of HZSM-5 are only 0.0162 mmol s$^{-1}$ and 0.101 mmol s$^{-1}$, respectively, at the same time point. The percentage increases in $CO_2$ desorption rate due to the use of $TiO(OH)_2$ and HZSM-5 catalysts as a function of time are presented in Fig. 1d. Remarkably, the increase in the rate of $TiO(OH)_2$ catalyzed $CO_2$ desorption can be as high as 4500%, while the highest increase in the rate of HZSM-5 catalyzed $CO_2$ desorption is only 750%. Therefore, $TiO(OH)_2$ can significantly catalyze $CO_2$ desorption, lower $CO_2$ desorption temperatures required for conventional $CO_2$ capture technologies, make $CO_2$ desorption occur at lower than 100 °C operable or practical, and significantly reduce the energy consumption of $CO_2$ capture. The further extended practical implication of the high $CO_2$ desorption rate could be its capability in reducing the dimension of amine scrubbing stripper for a given $CO_2$ capture task.

Figure 1e shows the effects of $TiO(OH)_2$ on the quantities of desorbed $CO_2$ within the same-time-length cycle of $CO_2$ sorption and desorption. The drastic enhancement in $CO_2$ desorption kinetics is illustrated in Fig. 1e with an increase in the total quantity $CO_2$ desorbed in the same time interval. Only 34.5 mmol

$CO_2$ is desorbed from the spent MEA solution when the catalyst was not used, and the increase of the amount of $CO_2$ desorbed is ~0% when $TiO_2$ is used. Silica gel shows a $CO_2$ desorption amount of 36.9 mmol, a ~7.0% increase. The HZSM-5 slightly improves $CO_2$ desorption amount to 39.2 mmol, only 14% increase. Extraordinarily, the presence of $TiO(OH)_2$ leads to a desorption of 64.1 mmol $CO_2$, about 86% increase. Although $TiO(OH)_2$ and HZSM-5 have similar surface areas (Supplementary Table 3), the improvement in the quantity of $CO_2$ desorption resulting from the use of $TiO(OH)_2$ is 430% higher than that with HZSM-5. It should be mentioned that the difference in $CO_2$ desorption amounts within a $CO_2$ sorption-desorption cycle should be much larger than 86% if $CO_2$ sorption is stopped when $CO_2$ sorption efficiency falls below DOE-target, 90%. Percentage increase in $CO_2$ desorption amount due to the use of $TiO(OH)_2$ and HZSM-5 are provided in Fig. 1f. In comparison with the $CO_2$ desorption of the uncatalyzed spent MEA, the cumulatively desorbed $CO_2$ quantity of the catalyzed spent MEA with $TiO(OH)_2$ is found to be 2500% higher than that of the uncatalyzed spent MEA at 771 s.

To avoid the impact of initial $CO_2$ loading difference on $CO_2$ desorption, the uncatalyzed and catalyzed $CO_2$ desorption studies started with two MEA solvents containing the same amount of $CO_2$ (~0.520 mol $CO_2$ mol$^{-1}$ MEA), which are achieved by absorbing $CO_2$ for 6000 s without the use of $TiO(OH)_2$. The desorption results without and with the use of $TiO(OH)_2$ are summarized in Supplementary Fig. 3 and Table 1. Clearly, the presence of $TiO(OH)_2$ catalyst is the main reason for the significantly accelerated $CO_2$ desorption, given that the initial $CO_2$ loadings in both spent MEA solvents are the same. The catalytic desorption profile of the spent MEA solvent shows a peak desorption rate of 0.183 mmol s$^{-1}$, 168% of the 0.109 mmol s$^{-1}$ achieved under uncatalyzed desorption condition. The increase in the $CO_2$ desorption rate resulting from the use of $TiO(OH)_2$ still can be as high as 2900% in comparison with that achieved without use of $TiO(OH)_2$. Accordingly, the total amount of desorbed $CO_2$ increases from 34.5 mmol to 53.5 mmol with the use of $TiO(OH)_2$ (Supplementary Fig. 3C).
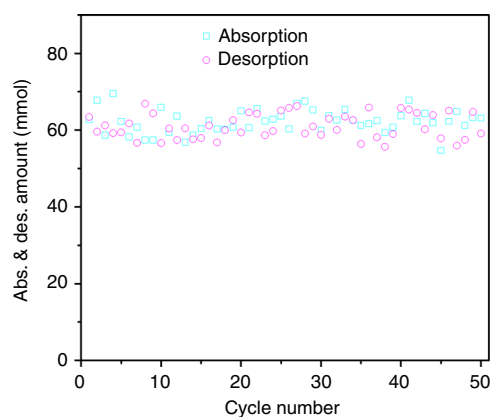


**Fig. 2** Catalyzed cyclic $CO_2$ absorption and desorption. The cyclic tests indicate the stability of $TiO(OH)_2$ under the given $CO_2$ absorption and desorption conditions. Absorption conditions—total mass of solution: 200 g; MEA concentration in the solution: 20 wt%; total flow rate of gas: 1000 mL/min; composition of gas: 10 vol% $CO_2$, 10 vol% $O_2$, and 80 vol% $N_2$; temperature: 25 °C; absorption time: 6000 and 3000 s for the 1st and 2nd–50th absorption tests, respectively. Desorption conditions—Total mass of solution: 200 g; MEA concentration in the solution: 20 wt%; temperature: 88 °C; time: 2400 s

**Catalyst and sorbent stability.** The stability of $TiO(OH)_2$ is assessed with 50 cycles of sorption-desorption tests. As shown in Fig. 2, no obvious decreases in both $CO_2$ sorption and desorption with the cyclic tests are observed. After cyclic tests, the spent catalyst is filtered, washed, dried, and then characterized by X-ray diffraction (XRD), thermogravimetric analysis (TGA), scanning electron microscope (SEM), and transmission electron microscope (TEM) (Supplementary Figs. 4–6). These characterization results prove that chemical structure of the $TiO(OH)_2$ is stable after 50 cyclic tests. The reason for the appearance of tiny XRD peaks of $TiO_2$ with the spent $TiO(OH)_2$ is not clear and need to be further studied. FT-IR result of the spent MEA solution (Supplementary Fig. 7) shows that MEA also remains stable during the cyclic tests, which may not be the case when it is exposed to the conventionally high regeneration temperatures.

**Raman spectroscopy.** Raman spectroscopy is used to investigate the catalytic effect of $TiO(OH)_2$ on both $CO_2$ sorption and desorption. To observe the impact of the catalyst on the sorption step, $CO_2$ sorption with and without $TiO(OH)_2$ for different sorption periods is performed. The corresponding Raman spectra of the spent MEA sorbents are measured and presented in Fig. 3a and b. The bonds at 1018 $cm^{-1}$, 1068 $cm^{-1}$, and 1160 $cm^{-1}$ are attributed to C–OH stretching of $HCO_3^-$, symmetric C–O stretching of $CO_3^{2-}$, and C–N stretching of $RNHCO_2^-$, respectively[17]. The peak height of $RNHCO_2^-$ generated under catalytic condition reached its highest point more quickly than that without use of the catalyst. Also, the peak intensity of $HCO_3^-$ at the end of the first 100 min of catalyzed $CO_2$ sorption is stronger than that obtained without use of catalyst. Both Raman spectra observations clearly demonstrate the great effect of the catalyst on $CO_2$ sorption. On the other hand, Raman spectra of the uncatalyzed and catalyzed $CO_2$ desorption tests for different periods
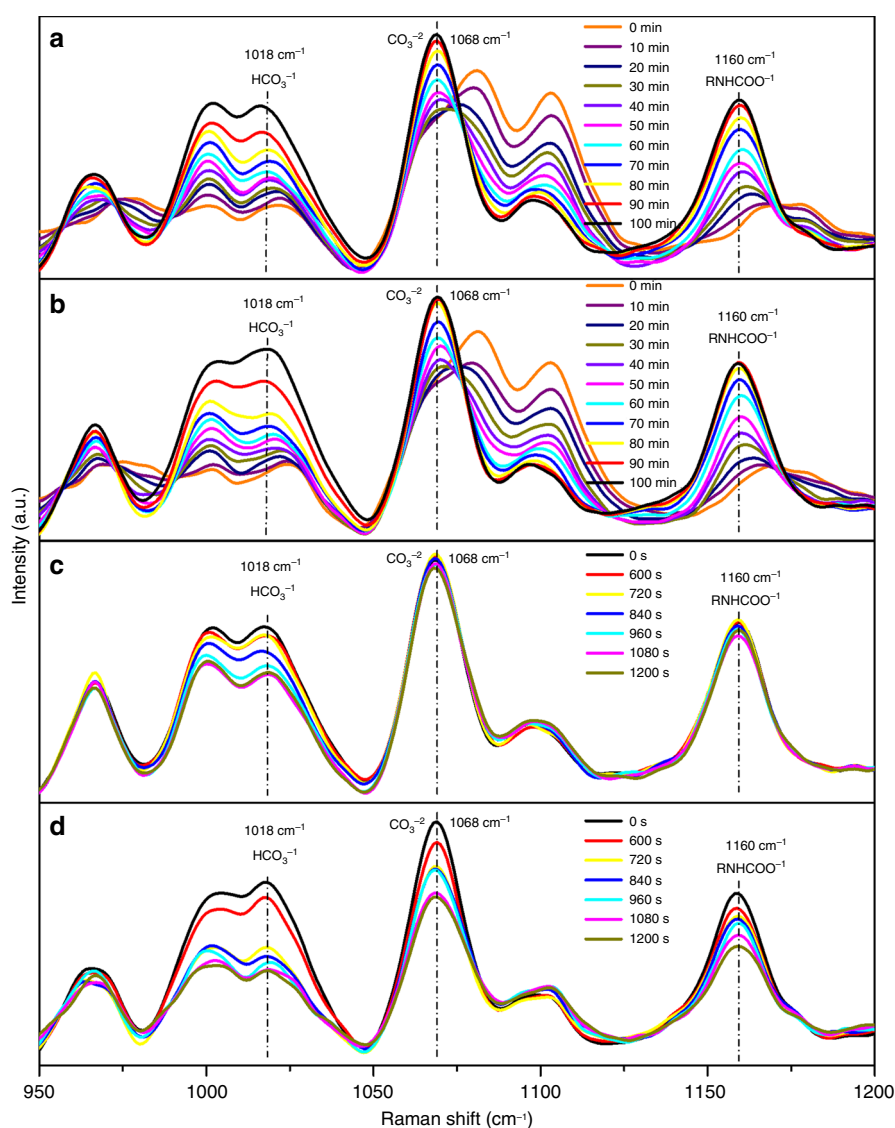


**Fig. 3** Raman spectra of solutions at different times. The indicated times are the periods when samples were taken during absorption and desorption tests for Raman spectrum analysis. The peak intensities are proportional to the concentration of species in solution. **a** $CO_2$ absorption without $TiO(OH)_2$, **b** $CO_2$ absorption with $TiO(OH)_2$, **c** $CO_2$ desorption without $TiO(OH)_2$, **d** $CO_2$ desorption with $TiO(OH)_2$. Absorption conditions—total mass of solution: 200 g; MEA concentration in the solution: 20 wt%; total flow rate of gas: 1000 mL/min; composition of gas: 10 vol% $CO_2$, 10 vol% $O_2$, and 80 vol% $N_2$; temperature: 25 °C; absorption time: 6000 s. Desorption conditions–total mass of solution: 200 g; MEA concentration in the solution: 20 wt%; temperature: 88 °C; time: 2400 s

(0–1200 s) are conducted and the spectra of the resulting MEA solutions are measured and shown in Fig. 3c and d to evaluate the catalytic enhancement effect of $TiO(OH)_2$. As can be seen from Fig. 3c, the peak intensity of $HCO_3^-$ in the uncatalyzed desorption derived MEA solution decreased gradually as $CO_2$ desorption continues, and that of $CO_3^{2-}$ and $RNHCO_2^-$ does not change during the first 840 s and then started to decrease at a much slower rate with desorption time. However, when desorption is catalyzed, all peak heights of $HCO_3^-$, $CO_3^{2-}$, and $RNHCO_2^-$ in the spent MEA solutions decrease at higher rates. The peak intensity of $HCO_3^-$ in the $TiO(OH)_2$-derived MEA solution becomes much weaker within just 720 s, a clear indication of a significant catalytic enhancement of $CO_2$ desorption due to $TiO(OH)_2$.

**Catalytic mechanism.** A possible catalytic mechanism for $TiO(OH)_2$-catalzyed MEA based $CO_2$ sorption and desorption is proposed in Fig. 4. There are three possible pathways for bicarbonate formation during $CO_2$ sorption and MEA regeneration ($CO_2$ desorption) (Supplementary Fig. 8). In the first pathway, forward and reverse steps a and b include carbamate ($MEACO_2^-$) generation via a zwitterion intermediate, and then bicarbonate formation through hydrolysis[18]. In the second pathway, one proceeds with forward and reverse formation of $(MEAH^+)(OH^-)$, and then bicarbonate, as shown in c

and d steps for $CO_2$ sorption and desorption, respectively. The last one essentially is the association and disassociation of carbonic acid (e and f steps). Protons transfers are directly associated with MEA based $CO_2$ absorption and desorption[18]. The hydroxyl group of $TiO(OH)_2$ with the ability of donating and accepting protons can greatly accelerate proton-involved reactions including protonation and deprotonation (Fig. 4). For example, $TiO(OH)_2$ can catalyze steps a and b by providing protons for MEA and accepting protons from zwitterion, which is beneficial to the formation of $MEAH^+$ and $MEACO_2^-$ during $CO_2$ sorption, while it provides protons for $MEACO_2^-$ decomposition and accepts protons for $MEAH^+$ deprotonation, which is favorable to sorbent regeneration or $CO_2$ desorption. Special attention should be paid to critical role of $TiO(OH)_2$ in the second and third pathways, in which the difficult direct proton transfer from $MEAH^+$ to $HCO_3^-$ is avoided via its proton donation to $HCO_3^-$ and deprotonation from $MEAH^+$.

**Methyl diethanolamine based sorbent.** To illustrate that the catalytic enhancement of $TiO(OH)_2$ is not unique to MEA, we use another common amine solvent methyl diethanolamine (MDEA), as an example, as shown in Supplementary Fig. 9. Comparing Fig. 1 and Supplementary Fig. 9 suggests that $TiO(OH)_2$ exhibits even stronger catalytic effect on $CO_2$ desorption
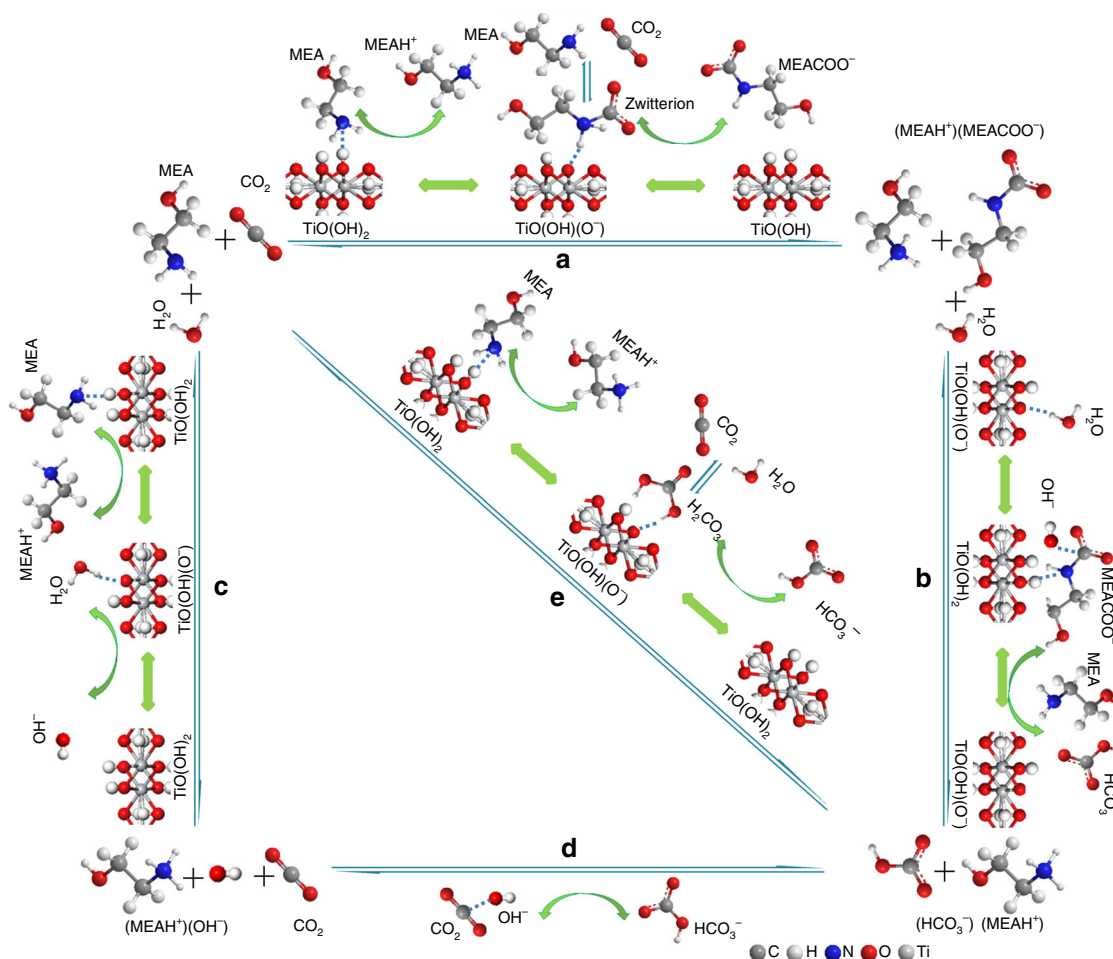


**Fig. 4** Proposed catalytic mechanism. Three possible pathways for $TiO(OH)_2$ to accelerate $CO_2$ absorption and desorption with MEA being a sorbent are presented. The hydroxyl group of $TiO(OH)_2$ accelerates both protonation and deprotonation reactions and thus $CO_2$ capture through reversible sorption and desorption via the special Lewis structure or the dual weak alkalinity and acidity of $TiO(OH)_2$

from MDEA. Only 2.12 mmol $CO_2$ is desorbed from the spent 20 wt% MDEA solution when the catalyst is not used. By contrast, the presence of $TiO(OH)_2$ leads to a desorption of 8.72 mmol $CO_2$, about 311% increase.

## Discussion

In summary, $TiO(OH)_2$ can significantly accelerate the both $CO_2$ sorption and desorption, and lower temperature and thus energy requirements for $CO_2$ capture. The alleviation in the capture conditions could lead to fundamental changes of people's passion for $CO_2$ emission control and successful fulfillment of Paris Agreement.

## Methods

**Preparation of TiO(OH)2**. Titanium isopropoxide was used as the precursor for preparing $TiO(OH)_2$ in this work. The first step was to add a predetermined amount of titanium isopropoxide into deionized (DI) water with a molar ratio of $H_2O$:Ti(O-iC$_3$H$_7$)$_4$ being 1400:1, followed by stirring the resulted mixture for 4 h. The precipitate powder was then filtered, rinsed three times with DI water and ethanol, then dried at 100 °C for ~10 h.

**Characterization**. The nitrogen physisorption at 77 K was performed on a Quantachrome Quadrasorb SI to determine the surface areas and pore structure of $TiO(OH)_2$. Powder X-ray diffraction (XRD) data were obtained by a Rigaku Smart Lab diffraction system with a Cu Kα radiation operated at 40 kV and 40 mA. Thermogravimetric analyses (TGA) of $TiO(OH)_2$ were performed on a TA Instruments SDT Q600 with a heating ramp of 10 °C min$^{-1}$. Fourier transform infrared (FTIR) spectroscopy spectra were collected on a Thermo Nicolet Magna-IR 760 spectrometer. Raman spectrum studies were conducted by using an Advantage 785 Raman Spectrometer with a 758 nm laser and up to 60 mW radiation power during measurement. The samples of MEA sorbents with different absorption and desorption times were prepared by taking about 1 ml solutions with a syringe at specific time, followed by filtering them with syringe filter to remove catalysts, and then placed them in clear shell vials for Raman measurements. Scanning electron microscopy (SEM) images of $TiO(OH)_2$ were obtained by using a FEI Quanta FEG 450 field-emission scanning electron microscope. Transmission electron microscopy (TEM) images of $TiO(OH)_2$ were taken by using a FEI Tecnai G2 F20 S-Twin 200 kV transmission electron microscope.

**CO2 capture**. $CO_2$ absorption and desorption studies were performed by using a setup schematically drawn in Supplementary Fig. 1. The reactor was a 500 mL glass reactor equipped with a magnetically coupled stirrer. In each sorption test, 200 g of 20 wt% MEA in water was used. Tests were done with or without catalyst. The concentrations (weight percentages) of catalysts varied from 1 wt% to 3 wt%.

$CO_2$ absorption experiment was done at room temperature (~25 °C) and atmospheric pressure (0.78 bar at Laramie in Wyoming). A total of 20 wt% MEA solution was prepared by mixing ethanolamine with deionized water. Predetermined amounts of 20 wt% MEA and catalyst were added into the reactor with a stirring rate of 600 rpm. The simulated flue gas containing 10 vol% $CO_2$, 10 vol% $O_2$, and 80 vol% $N_2$ was prepared by mixing individual gases. Three Parker mass flow controllers (Model 201) were used to accurately control the gas flow rates of $CO_2$ (99.99%), $O_2$ (99.999%), and $N_2$ (99.999%) from the corresponding cylinders. The simulated flue gas with a total flow of 1000 ml min$^{-1}$ was bubbled into MEA solution via a corrosion-resistant muffler (<100 μm, McMaster-Carr). The $CO_2$ concentration of the outlet gas of the reactor was measured with an inline gas analyzer (NDIR ZRE, California Analytical Instruments), and the measured concentration-time profile was recorded by a data recording unit. The quantity of $CO_2$ absorbed into MEA solution was calculated by integrating the recorded $CO_2$ sorption profiles. Upon the completion of absorption step taking 6000 and 3000 s for fresh and cyclic MEA solutions, respectively, the valve for inlet gas was closed.

$CO_2$ desorption was realized by heating the spent sorbent obtained from $CO_2$ sorption step to a desired desorption temperature (88 °C) gradually. The desorbed $CO_2$ went through a check valve and mixed with carrier gas ($N_2$) with a flow rate of 500 mL min$^{-1}$. The $CO_2$ concentration of the gas mixture was measured by an inline gas analyzer (NDIR ZRE, California Analytical Instruments). $CO_2$ concentrations in the gas mixture and the corresponding temperatures of the spent MEA solution were recorded in the whole $CO_2$ desorption process. Desorption test was stopped when the concentration of $CO_2$ in gas mixture was lower than 0.01%. It should be noted the vaporized MEA during $CO_2$ desorption operation was condensed and sent back to the reactor by using a condenser (#11 in Supplementary Fig. 1) along with a cooling unit (#13 in Supplementary Fig. 1). The following cyclic $CO_2$ sorption started to proceed when the temperature of regenerated MEA solution was cooled to 25 °C.

$CO_2$ absorption and desorption experiments with 20 wt% MDEA were conducted by using the same procedures as described earlier. In total 200 g of 20 wt% MDEA was used in the tests. After 6000 s of absorption, $CO_2$ desorption was realized by heating the spent MDEA sorbent to a desired temperature with the heating profile used for $CO_2$ desorption from spent MEA sorbent.

## References

1. Cox, P. M., Betts, R. A., Jones, C. D., Spall, S. A. & Totterdell, I. J. Acceleration of global warming due to carbon-cycle feedbacks in a coupled climate model. *Nature* **408**, 184–187 (2000).
2. Davis, S. J., Caldeira, K. & Matthews, H. D. Future $CO_2$ emissions and climate change from existing energy infrastructure. *Science* **329**, 1330–1333 (2010).
3. Haszeldine, R. S. Carbon capture and storage: how green can black be? *Science* **325**, 1647–1652 (2009).
4. Cui, S. et al. Mesoporous amine-modified $SiO_2$ aerogel: a potential $CO_2$ sorbent. *Energy Environ. Sci.* **4**, 2070–2074 (2011).
5. Rogelj, J. et al. Paris Agreement climate proposals need a boost to keep warming well below 2 °C. *Nature* **534**, 631–639 (2016).
6. UNFCCC. Adoption of the Paris Agreement. Report FCCC/CP/2015/L.9/Rev.1 (2015).
7. Rochelle, G. T. Amine scrubbing for $CO_2$ capture. *Science* **325**, 1652–1654 (2009).
8. Dutcher, B., Fan, M. H. & Russell, A. G. Amine-based $CO_2$ capture technology development from the beginning of 2013–a review. *ACS Appl. Mater. Interfaces* **7**, 2137–2148 (2015).
9. Yang, X. et al. Computational modeling and simulation of $CO_2$ capture by aqueous amines. *Chem. Rev.* **117**, 9524–9593 (2017).
10. Yu, C. H., Huang, C. H. & Tan, C. S. A review of $CO_2$ capture by absorption and adsorption. *Aerosol Air Qual. Res.* **12**, 745–769 (2012).
11. Dutcher, B., Fan, M. H. & Leonard, B. Use of multifunctional nanoporous TiO (OH)(2) for catalytic $NaHCO_3$ decomposition-eventually for $Na_2CO_3$/$NaHCO_3$ based $CO_2$ separation technology. *Sep Purif. Technol.* **80**, 364–374 (2011).
12. Dutcher, B. et al. Use of nanoporous FeOOH as a catalytic support for $NaHCO_3$ decomposition aimed at reduction of energy requirement of $Na_2CO_3$/$NaHCO_3$ based $CO_2$ separation technology. *J. Phys. Chem. C.* **115**, 15532–15544 (2011).
13. Liang, Z. W. et al. Experimental study on the solvent regeneration of a $CO_2$-loaded MEA solution using single and hybrid solid acid catalysts. *AIChE J.* **62**, 753–765 (2016).
14. Srisang, W. et al. Evaluation of the heat duty of catalyst-aided amine-based post combustion $CO_2$ capture. *Chem. Eng. Sci.* **170**, 48–57 (2017).
15. Bhatti, U. H. et al. Effects of transition metal oxide catalysts on MEA solvent regeneration for the post-combustion carbon capture process. *ACS Sustain Chem. Eng.* **5**, 5862–5868 (2017).
16. Figueroa, J. D., Fout, T., Plasynski, S., McIlvried, H. & Srivastava, R. D. Advances in $CO_2$ capture technology—The U.S. Department of Energy's Carbon Sequestration Program. *Int J. Greenh. Gas. Control* **2**, 9–20 (2008).
17. Wong, M. K., Bustam, M. A. & Shariff, A. M. Chemical speciation of $CO_2$ absorption in aqueous monoethanolamine investigated by in situ Raman spectroscopy. *Int J. Greenh. Gas. Control* **39**, 139–147 (2015).
18. Caplow, M. Kinetics of carbamate formation and breakdown. *J. Am. Chem. Soc.* **90**, 6795 (1968).

## Author contributions

Q.L. contributed to the idea, built the setup, synthesized catalyst, performed $CO_2$ capture, BET, XRD, SEM, TEM, TGA FT-IR, and Raman experiments, analyzed data and wrote the manuscript. S.T. performed Raman, assisted data analysis and manuscript writing. M. A.A. contributed towards the project idea and catalyst synthesis. H.C. assisted the setup building, $CO_2$ capture performance and cycle tests. A.G.R., H.A. and M.R. helped the

data analysis and manuscript writing. M.F. was involved in the project idea, supervision, results analysis and manuscript writing.

## Additional information

**Supplementary Information** accompanies this paper at https://doi.org/10.1038/s41467-018-05145-0.

**Competing interests:** The authors declare no competing interests.

**Reprints and permission** information is available online at http://npg.nature.com/reprintsandpermissions/

**Publisher's note:** Springer Nature remains neutral with regard to jurisdictional claims in published maps and institutional affiliations.